Vacuum 147 (2018) 134–142

Contents lists available at ScienceDirect

Vacuum

journal homepage: www.elsevier.com/locate/vacuum

Deposition of large area uniform diamond films by microwave plasma CVD

J. Weng [a], F. Liu [a, *], L.W. Xiong [a], J.H. Wang [a, b], Q. Sun [a]

[a] Key Laboratory of Plasma Chemistry and Advanced Materials of Hubei Province, Wuhan Institute of Technology, Wuhan 430205, China
[b] Institute of Plasma Physics, Chinese Academy of Sciences, Hefei 230031, China

ARTICLE INFO

Article history:
Received 29 September 2017
Received in revised form
19 October 2017
Accepted 19 October 2017
Available online 23 October 2017

Keywords:
Large area diamond film
High microwave power
Uniformity
Microwave plasma
Chemical vapor deposition

ABSTRACT

Diamond films with 70 mm in diameter were deposited on silicon substrates with $Ar/CH_4/H_2$ gas mixture, using microwave plasma chemical vapor deposition (MPCVD) technique. One designed water-cooling substrate stage was used to improve the uniformity of the surface temperature across the substrate. An uniform substrate surface temperature was obtained at the pressure of 10 kPa when the input microwave power was 5500 W. The condition of the plasma was diagnosed by optical emission spectrum (OES) and the grown diamond films were characterized by scanning electron microscopy (SEM), X-ray diffraction (XRD) and Raman spectroscopy. The results show that higher microwave power can further improve the uniformity of the temperature distribution across the substrate which in turn increases the uniformity of diamond film. And introducing more H_2 into $Ar/CH_4/H_2$ gas mixture at high microwave power is effective on the improvement of the quality and the decrease of the stress in the deposited diamond films. The diamond films with low average intrinsic stress of 0.32 GPa were finally deposited with introducing 100 sccm H_2 into $Ar/CH_4/H_2$ gas mixture at 5500 W.

© 2017 Elsevier Ltd. All rights reserved.

1. Introduction

Chemical vapor deposition (CVD) diamond film has received considered attentions and presented wide applications due to its excellent properties such as extreme mechanical hardness, high thermal conductive, wide band gap, negative electron affinity and chemical inertness [1–4]. Over the last two decades, there are more and more emphases on scale-up CVD techniques in order to satisfy industry requirements [5,6]. And the large area deposition of uniform diamond films by CVD method is considered as one of critical technological issues in the research and development (R&D) efforts [7,8].

Among all CVD methods for the preparation of diamond films, hot filament CVD (HFCVD) and microwave plasma CVD (MPCVD) are the most widely used ones to grow diamond films with various area, morphology and quality. Compared to the MPCVD technique, HFCVD is an easier and relatively lower cost way being used to uniform deposit diamond coatings on large area substrates by controlling the main parameters of substrate and filament temperature, carbon concentration and total deposition pressure. However, metal impurities produced by high temperature filaments can hardly be avoided in the deposition possess. Whereas the plasma generated by electrodeless discharge is much purer which makes MPCVD become the most suitable technique to prepare high quality diamond films [9]. For industry application, one technological barrier for MPCVD is the formation of a large uniform depositing area which is influenced by various factors such as electromagnetic filed distribution, substrate temperature variation, microwave power and distribution of active groups [10]. The correlation among the factors is complex, but they are restricted by a certain regulation that diamond films with similar quality can be obtained provided the power density of the plasma is similar [11]. In order to enlarge the uniform deposition area of MPCVD, researchers around the world pay many attentions on the design of different geometrical shaped chambers and the usage of high microwave power with lower frequency [10,12,13]. Füner et al. have reported development of an ellipsoidal shaped MPCVD chamber equipped with 2.45 GHz microwave source. And the MPCVD apparatus were following scaled up to 915 MHz one in which the diamond films with diameter from 50 mm to 120 mm have been prepared [14]. Their works on ellipsoidal geometry have been known Aixtron type MPCVD reactor commercially [15]. Yaran et al. have designed a 2.45 GHz quartz bell type MPCVD apparatus and

* Corresponding author.
E-mail address: smile_204@163.com (F. Liu).

https://doi.org/10.1016/j.vacuum.2017.10.026
0042-207X/© 2017 Elsevier Ltd. All rights reserved.

which is following scaled up by employing 915 MHz microwave energy to further enlarge the deposition area to 200 mm in diameter [16,17]. And the information of this type MPCVD apparatus can be referred from Lambda Technologies [17]. Cylindrical type MPCVD apparatus which is always equipped with 2.45 GHz microwave source have been designed nearly 20 years ago, and tremendous researches around the world have been carried out in this type of MPCVD system [18,19]. Nowadays, cylindrical type MPCVD apparatus can be commercially available in many companies. Seki Technotron, formally known as ASTeX, is a company focusing on designing CVD system which has been manufacturing MPCVD system since nearly 15 years ago. An overmoded MPCVD reactor have been designed which can generate larger scale plasma ball by utilizing two overlapped electromagnetic filed modes [20]. The diamond films with about 100 mm in diameter can be deposited in this type of MPCVD chamber when it is equipped with a 2.45 GHz microwave power [21]. By scaling up to 915 MHz, larger area diamond films with diameter of 150 mm can be obtained when a 60 kW microwave power is used [22]. Tachibana et al. also have detailed investigated the α parameters, the CVD conditions for morphology control and the diamond films texture in this 60 kW MPCVD system [23]. Recently, a novel geometric MPCVD chamber have been reported which points out that this type of MPCVD reactor can be equipped a 2.45 GHz microwave power and also can be scaled up to 915 MHz by adjusting the scale of chamber [8,24]. In this scaled-up MPCVD system, the diamond films with about 127 mm in diameter can be obtained [24].

There is a general conclusion that with the increase of the input microwave power and by reducing the frequency of microwave is an effective way to enlarge the deposition area. But it is not the case that large area diamond films with high quality can be prepared successfully with 915 MHz microwave unit, neither is it so that increasing microwave power can deposit a large area diamond films with high uniformity. There are still many processing issues should be addressed in order to govern the interactional multiple influential factors on the uniformity of diamond films. In this paper, the diamond films are deposited with $Ar/CH_4/H_2$ gas mixture in a 10 kW, 2.45 GHz MPCVD apparatus. And the morphology, the uniformity in thickness and quality as well as the intrinsic stress of the diamond films deposited at relative high microwave power and deposition pressure is detailed investigated. The experimental results is used as a guide to explore the deposition condition which is appropriate to improve the uniformity of diamond films, especially of microcrystalline diamond films.

2. Experimental details

2.1. MPCVD system

One self-made MPCVD reactor with 2.45 GHz and 10 kW microwave generator has been used for plasma formation. The schematic view of the reactor is shown in Fig. 1. And a detailed description of this type of MPCVD chamber has previously reported by our preliminary researches [9]. Microwave power is transmitted through a rectangular waveguide (BJ26) and coupled into the overmoded cavity by a coaxial antenna which is a cone-shaped inner conductor. Plasma processing takes place above the water-cooled copper stage which is located on the ring-shaped quartz window so that the damage of overheating and etching to the window can be reduced effectively. Two kinds of cooling tubes are set below the molybdenum substrate holder. The pipe diameter of the cooling tubes setting right below the center of substrate holder is bigger than that setting below the other areas. And the gap among the cooling tubes below the center of substrate holder is much smaller than that below the other areas. It has been observed that the arrangement of the cooling tubes can further reduce the surface temperature variation of substrate compared with Ref. [9]. During the deposition of CVD diamond films, the variation of the surface temperature across the substrate can be maintained lower than 65 °C at 10 kPa when the microwave power is set in the range from 3000 W to 6000 W. In such conditions, the surface temperature on the silicon substrate can be kept higher than 600 °C which is appropriate for the deposition of nanocrystalline and microcrystalline diamond films. Take one deposition condition for example, using the silicon wafer (1.0 mm in thickness and 60 mm in diameter) as the substrate, the average surface temperature of 800 °C with the variation of 47 °C across the substrate can be obtained at 10 kPa when the microwave power is 4600 W and the gas flow rate of $H_2/CH_4/Ar$ is 60/6/300. That is a desired surface temperature to deposit uniform diamond films. The height and the diameter of the molybdenum substrate holder are about 8 mm and 85 mm. The edge of the substrate holder is chamfered with radium of around 5 mm in order to eliminate the edge effect during deposition process.

Fig. 2 shows simulation results of the electric field distribution and the condition of Ar plasma generated by 5.0 kW at 13.0 kPa. It can be observed from the modeling result that for the distribution of electric filed as shown in Fig. 2(a), there is one maximum strength region on the substrate holder in where the dominant resonant microwave modes of TM_{01} and TM_{02} are overlapped. Meanwhile it is hardly to observe the phenomenon referred as "marginal discharge" at the peripheral region of substrate holder which is benefit to produce a uniformity of plasma [25]. Correspondingly, the electron density (n_e) of Ar plasma is shown in Fig. 2(b). One homogeneous plasma ball can be observed near above the substrate holder, and the diameter of the region where the electron density is higher than 6×10^{16} $1/m^3$ is around 70 mm that is the scale of the substrate being used in our investigation. Thus, the substrate holder has negligible effect on the distribution of electric field and the condition of the plasma generated on the substrate. The simulation results, in some degree, suggest that the deposition condition is benefit to uniform grow the diamond films with high quality because the peripherally inhomogeneous plasma is avoided and the high electron density can be obtained [26].

2.2. Growth of diamond films

In this study, mirror polished single crystal silicon (100) wafers with diameter of 70 mm and thickness of about 1.0 mm were used as the substrates. All the Si substrates were pre-treated by mechanical scratching with 0.5 μm diamond powders. Following the scratching, the substrates were ultrasonically cleaned with acetone, methanol and deionized water for 3–5 min respectively to remove any contaminants. And N_2 gas was used to dry Si substrates prior to the growth of diamond films. The growth parameters and the temperature variation across the substrates are listed in Table 1. Relative high temperature uniformity over a large area should be maintained across the substrate to deposit uniform diamond films, which can be obtained by adjusting the water pressure and velocity in the cooling tubes set below the substrate holder. Generally, the water pressure and velocity in the cooling tubes set in the center area is higher than that set in the other areas. The deposition pressure and microwave power are coupled to achieve a large plasma ball thoroughly covering the substrate which is also important to the uniformity of the temperature distribution across the substrate. And the microwave power absorption/reflection can be controlled to optimum state through adjusting three screw adjuster in order to produce and maintain the large scale plasma ball. It should be noted that the surface temperature variation across the substrate generated by high pressure and relative low

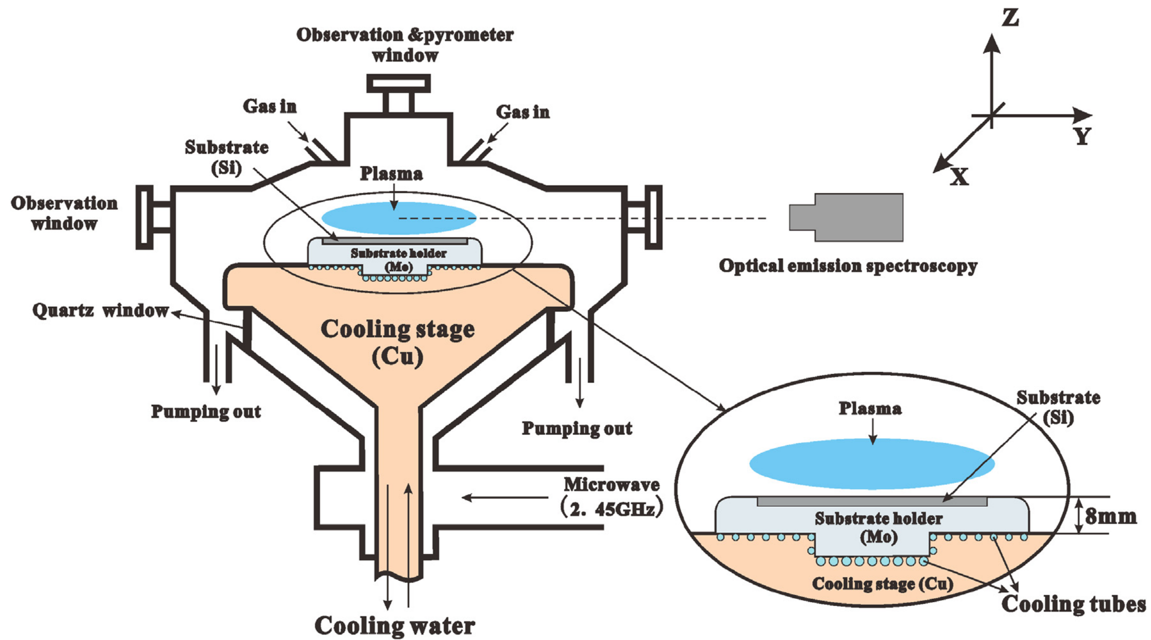

Fig. 1. Schematic diagram of the overmoded MPCVD reactor.

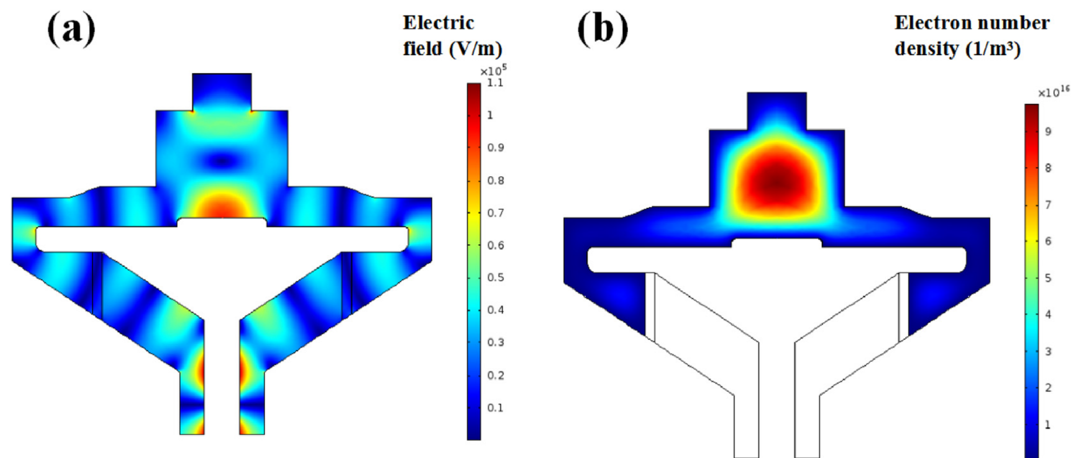

Fig. 2. Simulation results for (a) electric field intensity at 5000 W without plasma and electron number density of Ar plasma generated by 5000 W at 13 kPa.

Table 1
Deposition conditions for diamond films with 70 mm in diameter.

Samples	Microwave power (W)	Deposition pressure (kPa)	Ar flow rate (sccm)	CH_4 flow rate (sccm)	H_2 flow rate (sccm)	Average substrate temperature (°C)	Temperature variation (°C)
a	3000	10	300	6	60	720	57
b	5500				60	852	31
c	5500				100	857	42

microwave power can hardly be improved through adjusting the water pressure and velocity in the cooling tubes. The temperature of the growth surface on the different areas of substrate was monitored with a two-color infrared radiation thermometer (IRCON ULTIMAX™) during the deposition. The plasma characteristic were in-situ investigated with optical emission spectroscopy (OES) through a quartz window in the MPCVD chamber. The collected emission was directed to the spectrometer (Ocean Optics Maya2000 Pro) and the emission spectra along the X axis, parallel to the substrate, were record at ~10 mm above the substrate in this research. The total deposition time was kept constant for 6 h.

2.3. Characterization of diamond films

Surface morphology of the diamond films were characterized by scanning electron microscope (SEM, JSM-5510LV, Japan) which were also used to cross check the thickness and microstructure of growth diamond films. X-ray diffraction with CuK_α radiation (XRD,

D8ADVANCE, Germany) were used to evaluate the orientation and crystallographic texture of the diamond films. Raman spectroscopy (Raman, DXR, U.S.A.) with Ar laser operated at 514.5 nm was applied to characterize the phase purity and crystallinity of the grown coatings. And the intrinsic stress of the prepared diamond coatings were calculated with the shift of the diamond peak in Raman spectra.

3. Results and discussion

3.1. Optical emission spectroscopy

Optical emission spectroscopy is an effective method to detect the generated species produced by the decomposition of gas mixture which may influence the diamond growth directly, although OES can not identify all the radicals taking part in the diamond growth process [27]. Typical OES spectrum of microwave plasma in $H_2/CH_4/Ar$ gas mixture with different microwave power and hydrogen gas flow are shown in Fig. 3(a). The spectra were obtained at the distance Z is about 10 mm from substrate where is the center of the plasma. The atomic hydrogen lines H_α (656.5 nm) and H_β (486.1 nm) of Balmer series, atomic Ar peaks (696–850 nm), two strong C_2 Swan bands (516.5 nm and 557.8 nm) and the relatively weak CH band (431.4 nm and 432.4 nm) are present in the spectra. CN radicals (388.3 nm) are hardly detected which suggest the high vacuum during deposition.

It is well known that increasing input microwave power can leads to the increase of the number of active species which is benefit to improve the growth rate and quality [28]. In our experiment, the H_α line and C_2 Swan bands both increases with the microwave power. This phenomenon can be ascribed to the increased quantity of electrons and also by an increase in the quantity of the electrons which possess high enough energy to excite hydrogen atoms [29]. The further increased H_α line intensity is observed whereas the C_2 Swan bands intensity slightly decrease with the increase of H_2 concentration at the same microwave power. This effect, on the one hand, implies that the CVD diamond growth is very sensitive to the change in the hydrogen gas flow rate at relative high microwave power. On the other hand it suggests the energy of input microwave power set for the sample b and c is enough to excite more H atoms. And C_2 radicals can be kept at a relative constant concentration in the plasma because C_2 radicals possess lower excitation energy and longer lifetime compared to hydrogen atoms [29]. Therefore the increase of the microwave power and hydrogen gas flow in $Ar/CH_4/H_2$ is beneficial to improve the quality of CVD diamond films due to an increase in the H radicals which enhance the etching effect on non-diamond phases.

The analysis of the ratio between H_β and H_α is a sufficient approximation of T_e condition in the plasma. The results shown in Fig. 3(a) also present that the ratio of $I(H_\beta)/I(H_\alpha)$ in the center of plasma falls with the increase of microwave power and H_2 gas flow which indicates the decrease of T_e. This behavior may be one results of increased gas temperature (T_g). Higher microwave power increases the temperature of plasma which reduces the potential energy of electrons in the discharging area and produces more high-energy electrons, and also induces the thermal dissociation of hydrogen molecules [29]. That is one part of the reasons for the increase of atomic hydrogen. Increased electron concentration n_e is another reason at high microwave power, since the level of H_α line is mainly excited by electron impact and the intensity of $I(H_\alpha)$ is proportional to n_e [27]. A series of the spectra were recorded to evaluate the n_e distribution along the X axis, and the X-profile was obtained at the center of the plasma, as shown in Fig. 3(b). The X-profile for H_α intensity has a Gaussin shape and the increase of $I(H_\alpha)$ as a results from introducing more H_2 indicates an obvious increase of n_e in the plasma which is beneficial to the deposition of high quality diamond film [30]. An Abel inversion procedure can be applied to the $I(H_\alpha)$ profile to evaluate the radial distribution of local emissivity for $I(H_\alpha)$ which should be smaller than that observed on the photographs taken trough observation window [30]. And the $I(H_\alpha)$ profiling should be a more accurate way to estimate the plasma dimensions due to the direct relationship between electron density and diamond growth. In the $H_2/CH_4/Ar$ gas mixture used in our experiments, a large green plasma ball with diameter of 100 mm at least was observed through observation window. Meanwhile, the scale and the bright of the plasma ball increased with the input microwave power. The larger scale of the observed plasma ball lies in the gas diffusion and convection [27]. Thus, the scale of the selected substrates is much smaller than the observed plasma ball in order to ensure the electron concentration around the substrate and the uniformity of diamond films.

3.2. Surface morphology

The surface morphology of the diamond films deposited on the Si substrates were shown in Fig. 4. Fig. 4(a–c) show the surface morphology of samples a-c deposited for 0.5 h, and Fig. 4(d–f) show the final surface morphology of the corresponding samples. As shown in Fig. 4(a–c), scattered or merged diamond islands with various scale and morphology which are the nuclei for the growth of diamond films distribute on the scratch preferentially. The pretreatment of the three samples is the same, thus the nucleation condition on the substrate is mainly influenced by the parameters.

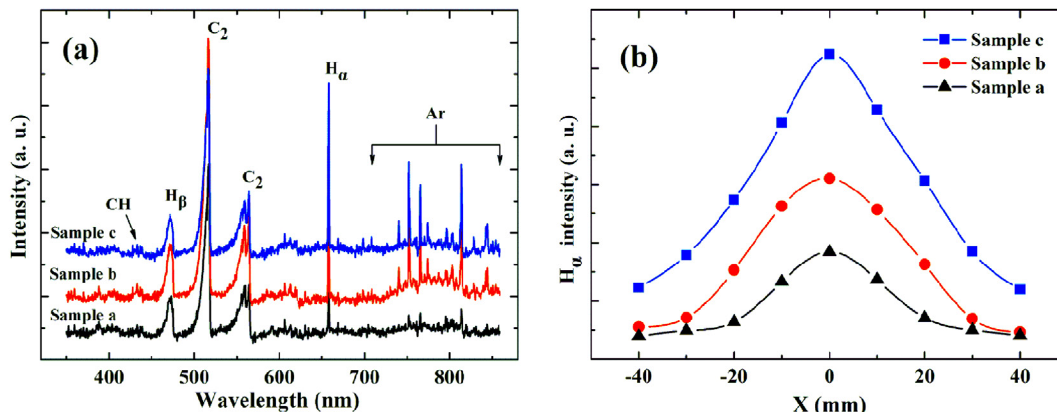

Fig. 3. Plasma diagnostic results for the samples: (a) OES spectra obtained at the center of the plasma, and (b) spatial profiles for H_α along X axis at the center of the plasma.

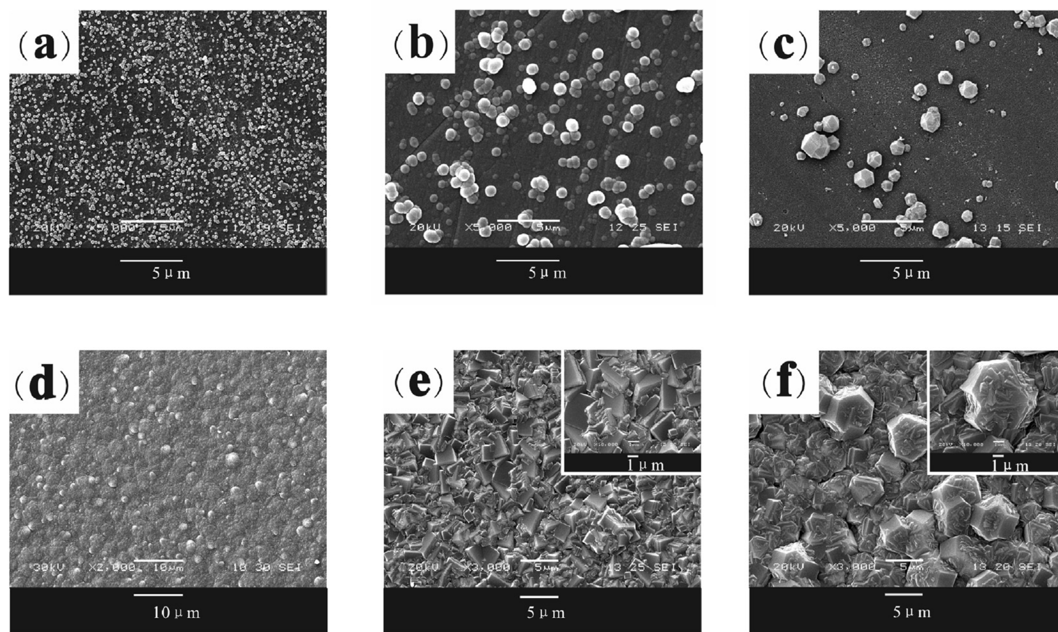

Fig. 4. SEM images of the samples deposited for 0.5 h: (a) sample a, (b) sample b, (c) sample c, and the final surface morphology of the samples after depositing 6 h: (d) sample a, (e) sample b, (f) sample c.

Compared with sample a, the nucleation density of the sample b and sample c is lower which is result from relative lower carbon supersaturation on the surface of substrate produced by higher substrate temperature [31]. Fig. 4(c) shows regular hexagon diamond islands which should possess relative higher quality than that of sample a and sample b. And the reason maybe the increased H radicals in the plasma which enhances the etching effect on non-diamond phases during precoalescence stage of diamond film growth and also leads to the improvement of the nucleation quality and the decrease of nucleation density. For the final morphology of diamond films, sample a possesses the smallest grain size, as shown in Fig. 4(e), because of the relative high carbon supersaturation on the surface of substrate. Meanwhile the relative high C_2 radicals in the plasma further enhance the re-nucleation effect during the diamond film growth. For the sample b, the substrate is coated with a continuous and dense diamond film, which consisted of relative well-defined (100) facets with disorderly arrangement. And some twins can be observed in the grain boundaries, as shown in Fig. 4(e). The SEM micrograph of sample c for the final morphology, as shown in Fig. 4(f), illustrates well-faceted diamond crystallites of which the average size is about 5 μm. In our experimental condition, the difference in the final morphology between sample b and sample c should be mainly attributed to the activated H radicals in the plasma. The increase of activated H concentration in the plasma enhances the etching effect on the non-diamond phases and also decreases nucleation density which is beneficial to increase the quality of diamond films as well as gives more gap among diamond nucleus being appropriate for the growth of diamond grains.

During the deposition of sample b and sample c, it also can be observed the phenomenon that there are diamond films depositing on the Mo substrate holder. Fig. 5 shows the SEM image of the deposited diamond film on the Mo substrate holder when depositing sample c. The polycrystalline nature of diamond film can be clearly seen and the surface morphology of this diamond film is consisted of (100) well-faceted diamond grains. The number of (100) facets on the region where have been chamfered (Arc region) is higher than that on the other regions, as shown in Fig. 5(a). The higher magnified SEM images of the diamond films on the Arc region and the other regions are shown in Fig. 5(b) and (c), respectively. The spiral morphology on the (100) facets can be observed of which the reason is the random nucleation on the (100) facets [11]. Besides that the reason of the differences in the grain scale and the number of (100) well-facet between the Arc region and the other regions is deduced that the electron density on the Arc region is higher than that on the other regions of the substrate holder, although chamfering have been carried out to eliminate the edge effect to the greatest extent.

3.3. Thickness

Three areas along the diameter lengths were chosen as shown in Fig. 6 for measuring thickness variation of the deposited diamond films over 70 mm diameter silicon substrate. Fig. 6 includes the thickness distribution of diamond films for three samples and the typical cross-sectional SEM of the nano-crystalline diamond film (sample a) as well as the micro-crystalline diamond films (sample b). And the thickness of the diamond films deposited on the Mo substrate holder when depositing sample b and sample c respectively are also present in Fig. 6. Sample a possesses the accumulation-growth mode indicating a relative lower growth rate and smaller grain size compared with that of sample b which has the columnar-growth mode. Sample a shows about 3.3 μm in thickness variation at a radial distance of 30 mm from the center of the substrate. Whereas, 2.1 μm variation in thickness is observed at 30 mm distance from the center of the substrate for sample b. Since there is a temperature variation from the center to the edge of the substrate, and it leads to the different growth rate of CVD diamond film at different areas. Comparing with the sample a and sample b, the increased microwave power should be the mainly factor for the increase of growth rate and the change of growth mode. The increased scale of plasma ball resulted from the increase of microwave power is the reason to decrease the temperature variation across the substrate which decreases the thickness variation of deposited diamond film. With the increase of H_2 gas flow rate, the

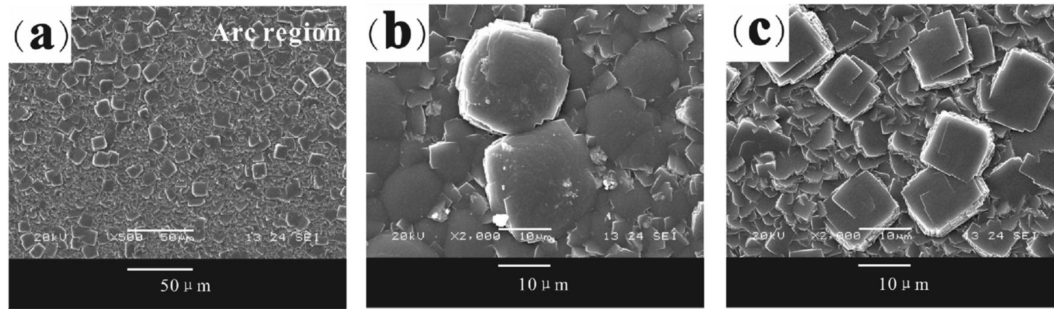

Fig. 5. SEM images of the diamond films on the Mo substrate holder when depositing sample c: (a) the diamond film deposited on the edge of the Mo substrate holder, (b) the diamond film in Arc region shown in (a), (c) the diamond film in the other regions shown in (a).

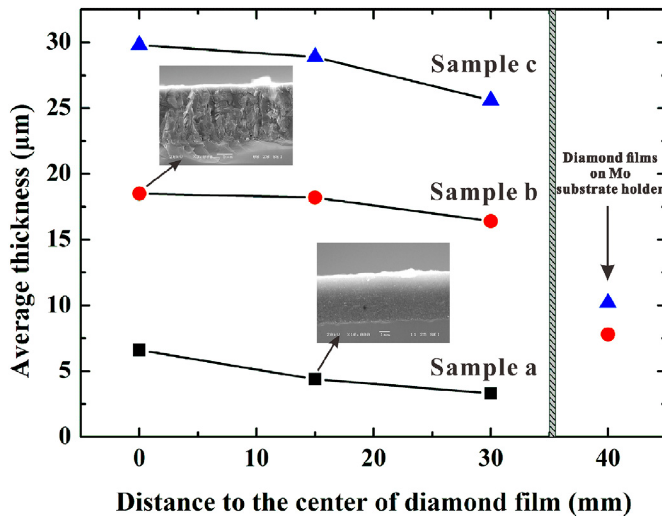

Fig. 6. Thickness variation of the diamond films deposited on Si substrates and the thickness of the diamond films deposited on Mo substrate holder. Insert SEM images are the cross-sectional morphology of sample a and sample b.

thickness variation across the substrate with 70 mm in diameter increases to 4.2 μm and the growth rate of CVD diamond film gets a further increase simultaneously. This behavior suggests that H_2 addition is significant to the growth rate, however, high microwave power is needed to ensure the large area deposition uniformity. Meanwhile, it is certain that applying high microwave power is necessary to increase the deposition area and uniformity of CVD diamond film. The thickness of the diamond films deposited on the Mo substrate holder using the parameters of sample b and c are 7.8 μm and 10.2 μm respectively which is lower than that deposited on the Si substrate. The reason lies in the spontaneous nucleation which results in a relative low growth rate.

3.4. Crystal structure

The crystal facets orientation of samples a, sample b and sample c were investigated by utilizing XRD, as shown in Fig. 7. There are two primary peaks can be observed at the diffraction angle 2θ of 43.74° and 74.14° for sample a shown in Fig. 7(a), which corresponds to (111) and (220) reflections of diamond films. And the average grain size are calculated with Sherrer's equation [32,33]: $d = 0.89\lambda/B\cos\theta$, where $\lambda = 0.1542$ nm and B is the full width at half maximum (FWHM) of (220) diffraction peak. The average grain size of sample a is 56.1 nm which further confirms the nano-crystalline nature. XRD patterns in Fig. 7(b and c) corresponding to sample b and sample c show relatively sharp and narrow diffraction peaks with 2θ values of 43.74°and 119.80°. These peaks is indexed to the (111) and (400) planes respectively which signifies better crystallinity of these samples compared with sample a. And it is obviously that the intensity of (400) peak for sample c in XRD pattern is stronger than that for sample b. The reason of the phenomenon should be ascribed to the increased gas flow rate of H_2 at high microwave power which increases the growth rate of CVD diamond film and results in the emergence of (100) facts [11].

3.5. Raman spectra

Raman spectroscopy was carried out to evaluate the phase purity and stress of the diamond films. Fig. 8 shows the Raman spectra of sample a to sample c. All the obvious Raman peaks for diamond films have been Lorentz fitted. The sloping background in all Raman spectra is due to the photoluminescence of graphite phase [34]. For sample a, Fig. 8(a) presents the typical nanocrystalline diamond film Raman spectrum. The boarding diamond peak at around 1332 cm^{-1}, non-diamond board peak at the Raman shift around of 1500 cm^{-1} and the peak at 1140 cm^{-1} which is attributed to the C-H bonds in a transpolyacetylene segments presenting at the grain boundaries and surfaces of diamond film [35] can be observed. The result confirms the nanocrystalline nature and also indicates the low crystalline of sample a. With the increase of microwave power, the Raman spectrum of sample b shows one sharp and narrow diamond peak, and the intensity of non-diamond peak decrease obviously as shown in Fig. 8(b), which indicates that sample b is of higher quality. With increasing the gas flow rate of hydrogen, the quality of the diamond film is further improved which is proved by the strong intensity of diamond peak and weak nano-diamond peak in the Raman spectrum shown in Fig. 8(c). It has been observed in the result of OES that increasing microwave power and hydrogen gas flow rate in $Ar/CH_4/H_2$ gas mixture can increase the electron density in the plasma which should be an effective way to increase the growth rate and improve the quality of diamond film by enhancing the etching effect on non-diamond phases. And the results of Raman spectra for samples a-c give a solid evidence.

3.6. Intrinsic stress

Concerning the diamond films with relative high quality, the Raman spectra of sample b and sample c both exhibit peak shift to higher wave numbers compared with the characteristic peak of stress-free diamond at 1332.5 cm^{-1} [36]. It reveals that the deposited diamond films on Si substrate possess compressive stress.

The intrinsic stress of diamond films generally comprises residual stress and thermal stress. The residual stress can be

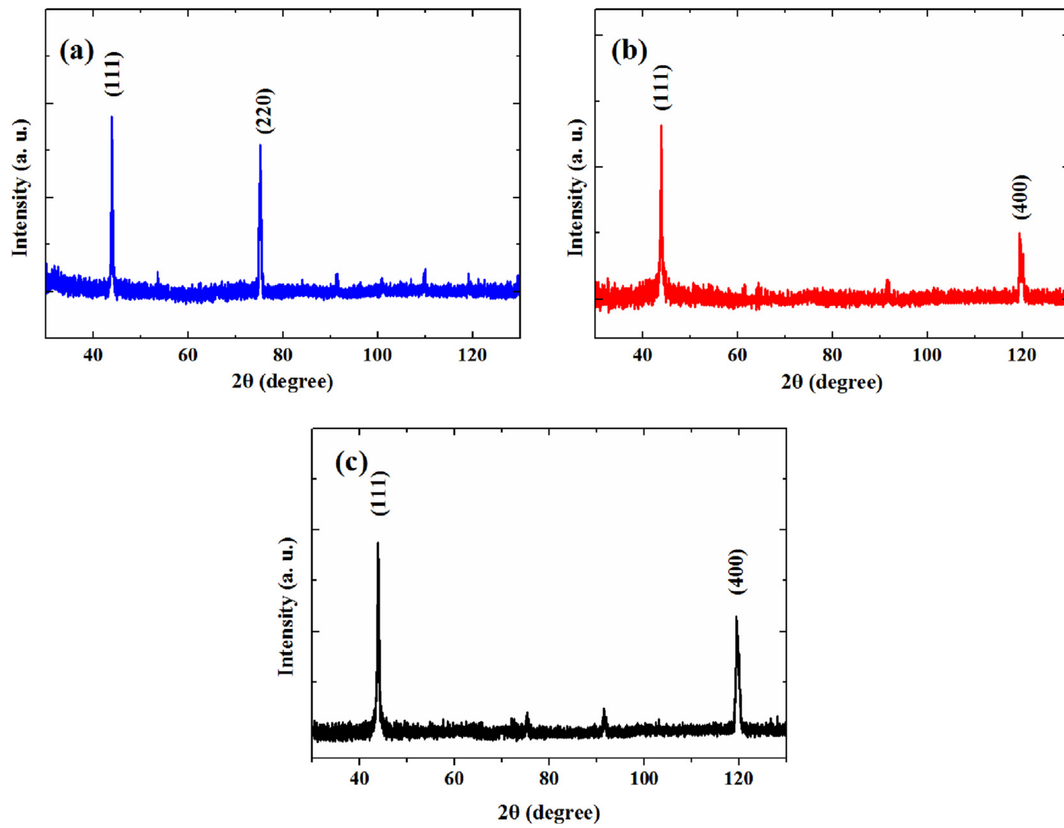

Fig. 7. XRD patterns of (a) sample a, (b) sample b and (c) sample c.

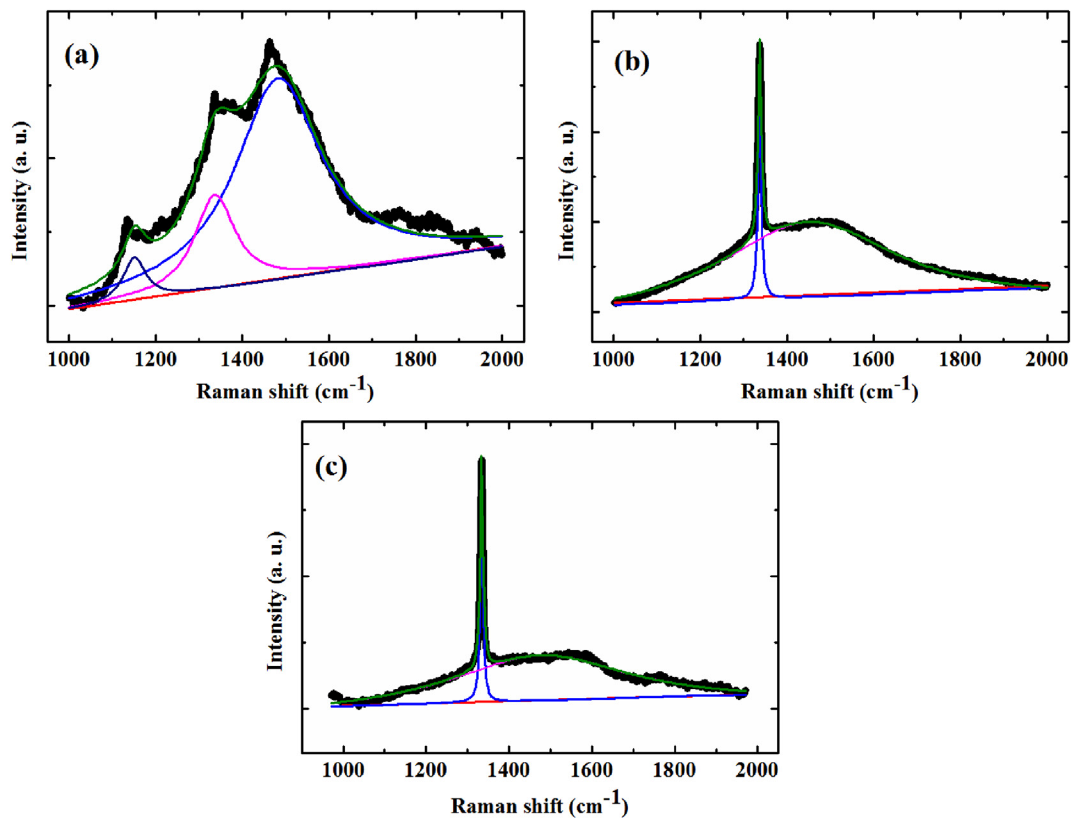

Fig. 8. Deconvolution of Raman spectra of diamond films: (a) sample a, (b) sample b, (c) sample c.

determined by Eq. (1) [36]:

$$\sigma_R = -0.617(\nu - \nu_0) \quad (1)$$

where $-0.617 GPa/cm^{-1}$ is the weighted average gauge factor for polycrystalline diamond, ν is the observed diamond peak position and $\nu_0 = 1332.5\ cm^{-1}$ which is the Raman peak shift for a stress-free diamond film. The thermal stress is produced in the stage of cooling. Thus the thermal stress can be calculated by Eq. (2) taking into account the thermal expansion mismatch between the diamond film and the Si substrate [37]:

$$\sigma_T = \frac{E}{1-\gamma}\int_{T_r}^{T}\left(\alpha_f - \alpha_s\right)dT \quad (2)$$

where E is the Young's modulus of microcrystalline diamond film (E = 1050 GPa), γ is the Poisson's ratio of diamond film (γ = 0.2), α_f and α_s are the coefficient of thermal expansion (CTE) of diamond film and Si substrate, respectively. T and T_r are the deposition temperature and the room temperature. In our investigation, samples b and sample c were both deposited at the substrate temperature around 850 °C and taken out after cooling to the room temperature about 25 °C. Thus, the CTE can be calculated using the following equation:

$$\alpha = \frac{\alpha_T + \alpha_{Tr}}{2} \quad (3)$$

where α_T and α_{Tr} are the value of CTE for the materials at the deposition temperature and the room temperature. For sample b and sample c, the value of α_f and α_s for the diamond coating and the Si substrate are $4.58 \times 10^{-6}/°C$ and $4.67 \times 10^{-6}/°C$ at deposition temperature, respectively. At room temperature, $\alpha_f = 1.15 \times 10^{-6}/°C$ and $\alpha_s = 3.58 \times 10^{-6}/°C$ for the samples. Based on the calculation, the thermal stress of the samples is −1.89 GPa. The intrinsic stress can be obtained using the following equation:

$$\sigma = \sigma_R + 1.89 \quad (4)$$

Fig. 9 represents the distribution of the intrinsic stress across the diamond film of sample b and sample c. The variation of the intrinsic stress of sample b is smaller than that of sample c. And the reason of the phenomenon lies in the surface temperature variation across the substrate. Employing higher microwave power can generate larger scale plasma ball at a certain deposition pressure which further decrease the temperature variation across the substrate placed on our designed water-cooling substrate holder. Increasing hydrogen gas flow rate in $Ar/CH_4/H_2$ gas mixture maybe results in an increase of the temperature variation across the substrate. And the increased hydrogen may also enhances the exothermic recombination of two hydrogen radicals to dihydrogen on the surface of substrate. This behavior should be a source of additional surface heating which plays a role in the increase of the surface temperature variation across the substrate and would affects the stress level in the films [38,39]. In our experiments, increased hydrogen concentration is beneficial to the increase of the electron density and the excited H atoms which can improve the quality and decrease the compress stress of diamond films. Thus, the average intrinsic stress for sample c is 0.32 GPa which is lower than that of sample b (−1.02 GPa), and the lower intrinsic stress is a favourable aspect to avoid the production of cracks in the deposition of diamond films.

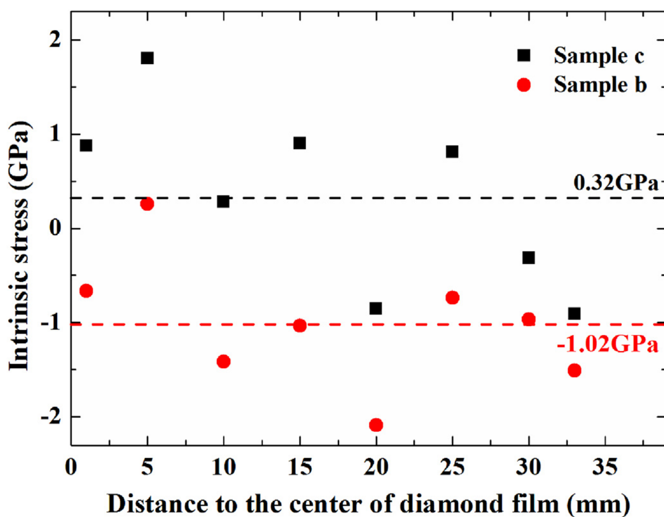

Fig. 9. Intrinsic stress of the sample b and sample c.

4. Conclusions

In present work, large area uniform diamond films with 70 mm in diameter were prepared in a home-made overmoded MPCVD reactor. One water-cooling substrate stage were designed to improve the uniformity of the surface temperature across the substrate. And the simulation results for the electrical distribution and the Ar plasma indicate that the deposition condition is benefit to grow uniform diamond films with high quality. Besides that the characterization results for the deposited diamond films show that with the increase of the microwave power to 5500 W, the high quality microcrystalline diamond film with the thickness variation of 2.1 μm is obtained due to the lower temperature variation across the substrate. Further increasing the H_2 gas flow in the $Ar/CH_4/H_2$ gas mixture is beneficial to the increase of growth rate and quality of diamond films at high microwave power because of the increased electron density in the plasma. And introducing more H_2 into $Ar/CH_4/H_2$ gas mixture also benefits the decrease of the stress of diamond films. The diamond films with low average intrinsic stress of 0.32 GPa were deposited when introducing 100 sccm H_2 into $Ar/CH_4/H_2$ gas mixture at 5500 W.

Acknowledgements

This work was supported by the Natural Science Foundation of China (grant numbers: 51402220), the Science and Technology Research Program of Hubei Education Department (grant numbers: Q20151517) and the Research Fund of Wuhan Institute of Technology (grant numbers: K201506).

References

[1] D. Liu, J. Xu, K. Gao, X. Kang, Investigations on etching resistance of undoped and boron doped polycrystalline diamond films by oxygen plasma etching, Vacuum 128 (2016) 80–84.
[2] V.V.S. Kumar, Nanocrystalline diamond films growth by microwave ECR CVD: studies of structural and photoconduction properties, Vacuum 131 (2016) 259–263.
[3] Q. Sun, J.H. Wang, J. Weng, F. Liu, Surface structure and electric properties of nitrogen incorporated NCD films, Vacuum 137 (2017) 155–162.
[4] P. Gautama, H. Toyota, Y. Iwamoto, X. Zhu, S. Nomura, S. Mukasa, Synthesizing diamond film on Cu, Fe and Si substrate by in-liquid microwave plasma CVD, Precis. Eng. 49 (2017) 412–420.
[5] J.J. Alcantar-Peña, E. Obaldi, J. Montes-Gutierrez, K. Kang, M.J. Arellano-Jimenez, J.E.O. Aguilar, G.P. Suchy, D. Berman-Mendoza, R. Garcia, M.J. Yacaman, O. Auciello, Fundamentals towards large area synthesis of multifunctional Ultrananocrystalline diamond films via large area hot filament chemical vapor deposition bias enhanced nucleation/bias enhanced growth for fabrication of broad range of multifunctional devices, Diam. Relat. Mater. 78 (2017) 1–11.

[6] Y. Ando, Y. Yokota, T. Tachibana, A. Watanabe, Y. Nishibayashi, K. Kobashi, T. Hirao, K. Oura, Large area deposition of <100>-textured diamond films by a 60-kW microwave plasma CVD reactor, Diam. Relat. Mater. 11 (2002) 596–600.
[7] E.M.A. Fuentes-Fernandez, J.J. Alcantar-Peña, G. Lee, A. Boulom, H. Phan, B. Smith, T. Nguyen, S. Sahoo, F. Ruiz-Zepeda, M.J. Arellano-Jimenez, Pablo Gurman, C.A. Martinez-Perez, M.J. Yacaman, R.S. Katiyar, O. Auciello, Synthesis and characterization of microcrystalline diamond to ultrananocrystalline diamond films via Hot Filament Chemical Vapor Deposition for scaling to large area applications, Thin Solid Films 603 (2016) 62–68.
[8] Y.F. Li, X.M. An, X.C. Liu, L. Jiang, P.W. Zhang, H. Guo, Z.L. Sun, H.Z. Zhao, W.Z. Tang, A 915 MHz/75 kW cylindrical cavity type microwave plasma chemical vapor deposition reactor with a ladder-shaped circumferential antenna developed for growing large area diamond films, Diam. Relat. Mater. 78 (2017) 67–72.
[9] J. Weng, L.W. Xiong, J.H. Wang, S.Y. Dai, W.D. Man, F. Liu, Investigation of depositing large area uniform diamond films in multi-mode MPCVD chamber, Diam. Relat. Mater. 30 (2012) 15–19.
[10] A.K. Mallik, S. Bysakh, K.S. Pal, N. Dandapat, B.K. Guha, S. Datta, D. Basu, Large area deposition of polycrystalline diamond coatings by microwave plasma CVD, Trans. Indian Ceram. Soc. 72 (2013) 225–232.
[11] J. Weng, J.H. Wang, S.Y. Dai, L.W. Xiong, W.D. Man, F. Liu, Preparation of diamond films with controllable surface morphology, orientation and quality in an overmoded microwave plasma CVD chamber, Appl. Surf. Sci. 276 (2013) 529–534.
[12] Y. Yokota, Y. Ando, A. Watanabe, Y. Nishibayashi, K. Kobashi, T. Hirao, K. Oura, Growth of <100> oriented polycrystalline diamond films of 6 inch diameter, New Diam. Front. Carbon Technol. An Int. J. New Diam. Front. Carbon & Relat. Mater. 12 (2002) 117–120.
[13] A.K. Mallik, K.S. Pal, N. Dandapat, B.K. Guha, S. Datta, D. Basu, Influence of the microwave plasma CVD reactor parameters on substrate thermal management for growing large area diamond coatings inside a 915 MHz and moderately low power unit, Diam. Relat. Mater. 30 (2012) 53–61.
[14] M. Funer, C. Wild, P. Koidl, Novel microwave plasma reactor for diamond synthesis, Appl. Phys. Lett. 72 (1998) 1149–1151.
[15] F. Silva, K. Hassouni, X. Bonnin, A. Gicquel, Microwave engineering of plasma-assisted CVD reactors for diamond deposition, J. Phys. Condens. Matter An Inst. Phys. J. 21 (2009) 364202.
[16] S.S. Zuo, M.K. Yaran, T.A. Grotjohn, D.K. Reinhard, J. Asmussen, Investigation of diamond deposition uniformity and quality for freestanding film and substrate applications, Diam. Relat. Mater. 17 (2008) 300–305.
[17] D. King, M.K. Yaran, T. Schuelke, T.A. Grotjohn, D.K. Reinhard, J. Asmussen, Scaling the microwave plasma-assisted chemical vapor diamond deposition process to 150-200 mm substrates, Diam. Relat. Mater. 17 (2008) 520–524.
[18] J. Weng, L.W. Xiong, J.H. Wang, W.D. Man, G.H. Chen, Effect of gas sources on the deposition of nano-crystalline diamond films prepared by microwave plasma enhanced chemical vapor deposition, Plasma Sci. Technol. 12 (2010) 761–764.
[19] Y. Ando, T. Tachibana, K. Kobashi, Growth of diamond films by a 5-kW microwave plasma CVD reactor, Diam. Relat. Mater. 10 (2001) 312–315.
[20] T. Ochiai, K. Arihara, C. Terashima, A. Fujishima, Electrochemical reduction of ozone dissolved in perchloric acid solutions at boron-doped diamond electrodes, Chem. Lett. 35 (2006) 1018–1019.
[21] A.C. Taylor, B. Vagaska, R. Edgington, C. Hébert, P. Ferretti, P. Bergonzo, R.B. Jackman, Biocompatibility of nanostructured boron doped diamond for the attachment and proliferation of human neural stem cells, J. Neural Eng. 12 (2015) 066016.
[22] T. Tachibana, Y. Ando, A. Watanabe, Y. Nishibayashi, K. Kobashi, T. Hirao, K. Oura, Diamond films grown by a 60-kW microwave plasma chemical vapor deposition system, Diam. Relat. Mater. 10 (2001) 1569–1572.
[23] Y. Yokota, Y. Ando, K. Kobashi, T. Hirao, K. Oura, Morphology control of diamond films in the region of α=1-1.5 using a 60-kW microwave plasma CVD reactor, Diam. Relat. Mater. 12 (2003) 295–297.
[24] Y.F. Li, J.J. Su, Y.Q. Liu, M.H. Ding, X.L. Li, G. Wang, P.L. Yao, W.Z. Tang, Design of a new TM_{021}, mode cavity type MPCVD reactor for diamond film deposition, Diam. Relat. Mater. 44 (2014) 88–94.
[25] R.A. Akhmedzhanov, A.L. Vikharev, A.M. Gorbachev, V.A. Koldanov, D.B. Radishchev, Studies of pulse operation regime of microwave plasma CVD reactor, Diam. Relat. Mater. 11 (2002) 579–583.
[26] A.N. Kang, L. Chen, J. Liu, Y. Zhao, X.B. Yan, C.Y. Hua, J.C. Guo, J.J. Wei, L.F. Hei, C.M. Li, F.X. Lu, The effect of substrate holder size on the electric field and discharge plasma on diamond-film formation at high deposition rates during MPCVD, Plasma Sci. Technol. 19 (2017) 095505.
[27] J. Ma, M.N.R. Ashfold, Y.A. Mankelevich, Validating optical emission spectroscopy as a diagnostic of microwave activated $CH_4/Ar/H_2$ plasmas used for diamond chemical vapor deposition, J. Appl. Phys. 105 (2009) 1489–1581.
[28] T. Tachibana, Y. Ando, A. Watanabe, Y. Nishibayashi, K. Kobashi, T. Hirao, K. Oura, Large area deposition of N100M-textured diamond films by a 60-kW microwave plasma CVD reactor, Diam. Relat. Mater. 11 (2002) 596–600.
[29] S.A. Linnik, A.V. Gaydaychuk, Application of optical emission spectroscopy for the determination of optimal CVD diamond growth parameters in abnormal glow discharge plasma, Vacuum 103 (2014) 28–32.
[30] A.P. Bolshakov, V.G. Ralchenko, V.Y. Yurov, A.F. Popovich, I.A. Antonova, A.A. Khomich, E.E. Ashkinazi, S.G. Ryzhkov, A.V. Vlasov, A.V. Khomich, High-rate growth of single crystal diamond in microwave plasma in CH_4/H_2 and $CH_4/H_2/Ar$ gas mixtures in presence of intensive soot formation, Diam. Relat. Mater. 62 (2016) 49–57.
[31] J. Achard, F. Silva, O. Brinza, A. Tallaire, A. Gicquel, Coupled effect of nitrogen addition and surface temperature on the morphology and the kinetics of thick CVD diamond single crystals, Diam. Relat. Mater. 16 (2007) 685–689.
[32] C. Liu, J.H. Wang, J. Weng, Growth of micro- and nanocrystalline dual layer composite diamond films by microwave plasma CVD: influence of CO_2, concentration on growth of nano-layer, J. Cryst. Growth 410 (2015) 30–34.
[33] C. Hua, X. Yan, J. Wei, J.C. Guo, J.L. Liu, L.X. Chen, L.F. Hei, M. Li, Intrinsic stress evolution during different growth stages of diamond film, Diam. Relat. Mater. 73 (2017) 62–66.
[34] N.G. Ferreira, E. Abramof, N.F. Leite, E.J. Corat, V.J. Trava-Airoldi, Analysis of residual stress in diamond films by x-ray diffraction and micro-Raman spectroscopy, J. Appl. Phys. 91 (2002) 2466.
[35] Y.S. Zou, Z.X. Li, Y.F. Wu, Deposition and characterization of smooth ultrananocrystalline diamond film in $CH_4/H_2/Ar$ by microwave plasma chemical vapor deposition, Vacuum 84 (2010) 1347–1352.
[36] Z. Xu, L. Lev, M. Lukitsch, A. Kumar, Analysis of residual stresses in diamond coatings deposited on cemented tungsten carbide substrates, J. Mat. Res. 22 (2007) 1012–1017.
[37] X. Liu, Q. Wei, Z. Yu, T. Yang, H. Zhai, Adherent diamond film deposited on Cu substrate by carbon transport from nanodiamond buried under Pt interlayer, Appl. Surf. Sci. 265 (2013) 714–719.
[38] Y.Y. Xia, M.W. Zhao, F. Li, B.D. Huang, Z.Y. Tan, X.D. Liu, Y.J. Ji, L.M. Mei, Recombination and exchange reactions of hydrogen and dihydrogen molecular condensation in single-walled carbon nanotubes, J. Phys. Chem. B 108 (2004) 4711–4715.
[39] K. Makihara, M. Ikeda, T. Okada, S. Miyazaki, Application of remote hydrogen plasma to selective processing for Ge-based devices: crystallization, etching, and metallization, Jpn. J. Appl. Phys. 53 (2014), 11RA02.